



ELSEVIER

Palaeogeography, Palaeoclimatology, Palaeoecology 200 (2003) 187–205

PALAEO

www.elsevier.com/locate/palaeo

Response of Early Cretaceous carbonate platforms to changes in atmospheric carbon dioxide levels

Lukas Wissler, Hanspeter Funk, Helmut Weissert*

Geological Institute, ETH Zürich, 8092 Zürich, Switzerland

Received 21 December 2001; accepted 21 March 2003

Abstract

During the Late Barremian and Early Aptian (about 120 million years ago) intense volcanic degassing and extremely rapid release of methane hydrates contained in marine sediments added high amounts of carbon to the ocean and atmosphere, and resulted most probably in rising atmospheric carbon dioxide pressure. In order to document the response of the shallow water carbonate-producing communities to this pronounced disturbance of the carbon cycle we studied a Late Barremian to Early Aptian neritic carbonate succession deposited on the northern Tethyan shelf (Swiss Alps). The sedimentological and stable carbon and oxygen isotope records of two sections located along a N–S transect from proximal to more distal shelf environments were investigated. The sediments correspond to outer-, mid-, and inner-ramp deposits of a homoclinal carbonate ramp. Vertical facies variations within the two studied sections feature three progradation phases of the platform. A highly resolved correlation of the shelf sediments with a pelagic succession from the Southern Alps (Northern Italy) is based on both $\delta^{13}\text{C}$ stratigraphy and biostratigraphy, and indicates that the drowning of the Helvetic carbonate platform coincided with a pronounced calcification crisis of calcareous nannofossils. The biocalcification crisis started before but culminated during the Aptian methane event recorded in a negative carbon-isotope spike. We propose that increased carbon dioxide concentrations in oceans and atmosphere related to volcanic activity and to sudden methane release reduced the marine calcium carbonate oversaturation and the calcification potential of benthic and planktonic organisms. Carbonate-producing shallow water communities on platforms and ramps suffering from additional environmental stress such as extreme temperatures or high nutrient levels could not survive during times of rising sea level, and, as a consequence, carbonate platforms drowned.

© 2003 Elsevier B.V. All rights reserved.

Keywords: Carbonate platform; biocalcification; Early Cretaceous; carbon dioxide; carbon isotopes

1. Introduction

The growth and demise of reefs and carbonate

platforms strongly interact with the Earth's climate. Carbonates play a key role in the global carbon cycle as they represent the most important sink for carbon and alkalinity which is delivered to the ocean and atmosphere by volcanic degassing and by the chemical weathering of ancient rocks. In contrast, coastal carbonate ecosystems react sensitively to environmental and climatic

* Corresponding author. Tel.: +41-1-632-3715;

Fax: +41-1-632-1380.

E-mail address: helmut.weissert@erdw.ethz.ch
(H. Weissert).

changes, since organisms precipitating calcite and aragonite need specific ecological conditions to survive. The interaction between atmospheric $p\text{CO}_2$ and the marine carbonate system is the object of several recent studies dealing with the consequences of the currently rising atmospheric carbon dioxide concentration. Laboratory experiments as well as numeric modelling results predict a pronounced crisis in planktonic and neritic carbonate production in the next decades as a consequence of higher atmospheric CO_2 pressure (Gattuso et al., 1998; Kleypas et al., 1999; Gattuso and Buddemeier, 2000; Riebesell et al., 2000). We chose this prediction of a future carbon dioxide-induced biocalcification crisis as a starting point for our reconstruction of the growth and collapse of a Cretaceous carbonate platform. We examine whether the demise of Barremian–Aptian carbonate platforms (Weissert et al., 1998) correlates with major perturbations of global carbon cycling as monitored in the carbonate carbon-isotope record. Of peculiar interest is the question if a distinct negative carbon-isotope anomaly of Early Aptian age correlates with the growth crisis of the Aptian carbonate platforms. The negative carbon-isotope pulse preserved in the Early Aptian organic and carbonate carbon-isotope curve has been related to accelerated carbon dioxide fluxes caused by rising volcanic activity and/or by a rapid methane release from gas hydrates contained in marine sediments (Menegatti et al., 1998; Jenkyns and Wilson, 1999; Hesselbo et al., 2000; Groecke, 2002).

Growth crises of Early Aptian (ca 121–118 Myr) carbonate platforms are documented from the northern Tethys margin in the Swiss Alps (Funk et al., 1993; Föllmi et al., 1994), in the southeastern part of France (Arnaud-Vanneau and Arnaud, 1990; Masse, 1993; Hunt and Tucker, 1993), in southern Italy (Bosellini et al., 1999) and in southeastern Spain (Ruiz-Ortiz and Castro, 1998), but also from the Atlantic platforms along the eastern coast of North America (Jansa, 1993) as well as from the Texan and Mexican platform system (Scott, 1993; Wilson and Ward, 1993; Lehman et al., 1998). Less affected by the crisis were several platforms along the southern margin of the Tethys, for example parts of the

Arabian platform and the interior part of the Adriatic platform (Pratt and Smewing, 1993; Alsharan and Nairn, 1993; D'Argenio et al., 1993; Grötsch et al., 1998). For this study we chose to investigate the growth pattern of a northern Tethyan carbonate ramp which today is outcropping in the Helvetic Alps of northern Switzerland (Föllmi et al., 1994). By tracing the evolution of this carbonate ramp through the Barremian into the Early Aptian we could compare environmental conditions during the time of apparently undisturbed carbonate production with conditions existing during the time of carbonate ramp collapse. We used carbon-isotope stratigraphy, combined with sequence stratigraphy and biostratigraphy as a stratigraphic correlation tool and we interpreted the carbon-isotope curve as a tracer of global carbon cycling. We chose the well-documented Barremian–Aptian C-isotope record in the Southern Alps of Northern Italy (Menegatti et al., 1998; Erba et al., 1999) as a reference section for this investigation. The Italian section has been isotopically calibrated with the sections near historical stratotypes in southern France (Wissler et al., 2002).

2. Regional geology and studied sections

The studied shelf series were deposited on a carbonate ramp along the northern margin of the alpine Tethys Ocean. Today, they are located in the southern part of the Helvetic Säntis nappe of eastern Switzerland (Fig. 1A; Funk et al., 1993) and form the Drusberg and Schratzenkalk formations of the Helvetic Alps. The sediments considered contain a succession of Barremian to Lower Aptian inner and outer platform carbonates deposited on the northern shelf of the Early Cretaceous Tethys ocean (Fig. 1B). The base of the studied profiles is characterised by a condensed, glauconitic horizon (Altmann beds) dated with ammonites as latest Hauterivian and early Barremian (*angulicostata*–*caillaudianus* ammonite zones; Funk et al., 1993). The top of the investigated succession is overlain by the phosphoritic Upper Aptian Luitere bed (*crassicostatum* to *melchioris* ammonite zone; Ouwehand, 1987). Ten

kilometres north of the study area the topmost beds of the Schrattekalk Formation have been dated with benthic foraminifera to be of Early Aptian age (*Orbitolinopsis buccifer*, *O. briacensis*, *O. cuvillieri*, *O. pygmaea*; see Bollinger, 1988), similar to the uppermost sediments of the Urgonian carbonate platform in the Subalpine Chains (Arnaud et al., 1998).

The main section used for comparison consists of Hauterivian to Aptian pelagic carbonates deposited on the southern Tethyan margin. It was drilled by the APTICORE project into the Majolica and Scaglia formations close to the river Cison in the Southern Alps of Northern Italy (Fig. 1, Erba and Larson, 1998). Erba et al. (1999) describe the biostratigraphy, magnetostratigraphy and stable carbon-isotope stratigraphy of this drill core.

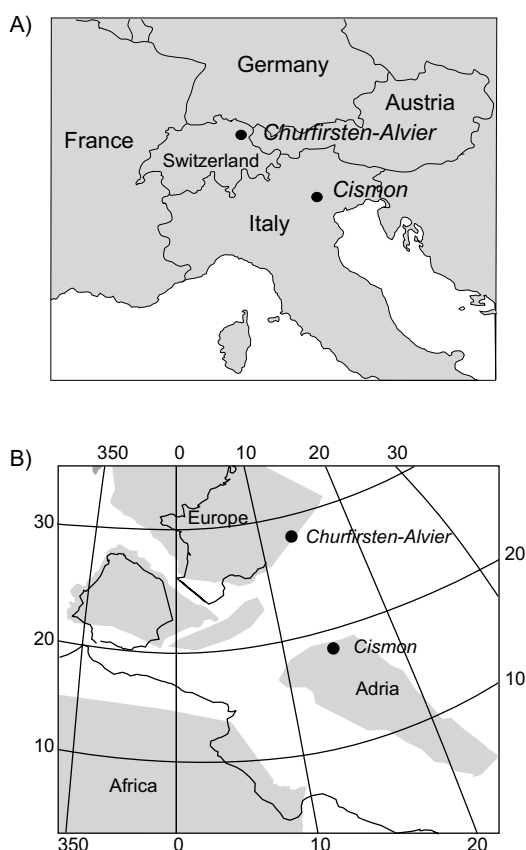


Fig. 1. Geographical (A) and palaeogeographical (B) map (Wortmann et al., 2001) of the study area and locations of the considered sections.

3. Methods

For this study we analysed two sections in different palaeogeographic positions along the northern Tethyan carbonate ramp. The more proximal Churfirsten section contains dominantly inner platform sediments. The more distal Alvier section is situated approximately 5–10 km towards the south and consists of mid- and outer-ramp deposits. The Churfirsten section has been measured and the sedimentological features and fossil content have been documented bed by bed in the field. Samples have been taken about every 2 m. Thin sections, peels and polished surfaces have been used for the microscopic description of the samples. The lithologic log and the sedimentological data of the Alvier section as well as the samples of the upper part of this profile (Glaenli) are taken from Briegel (1972). The lower part (Riseten) has been sampled by one of the authors (L.W.).

The isotopic composition of calcite was measured on bulk rock samples from limestones, marly limestones and marls. Carbonate powder was extracted with a microdrill in order to avoid diagenetic calcite from veins and large fossil fragments. The sampled material was reacted with 100% phosphoric acid and the carbon- and oxygen-isotope composition of the evolving CO₂ gas was analysed with a Prism dual-inlet mass spectrometer. The results are expressed in the common δ -notation in permil relative to the VPDB (Vienna PeeDee Belemnite) standard. Replicate analyses of selected samples have a reproducibility of approximately $\pm 0.1\text{‰}$ for $\delta^{13}\text{C}$ and $\pm 0.2\text{‰}$ for $\delta^{18}\text{O}$. For the stratigraphic correlation a three-point moving average was calculated which smoothed carbon-isotope profiles.

4. Results

4.1. Alvier

4.1.1. Sedimentology

Samples, lithologic log and sedimentological description of the Alvier section are taken from Briegel (1972). The results are presented in Figs. 2

and 3. The lower part of the section has been studied at the locality Riseten (Swiss coordinates: 748.525/222.050 base, 748.625/222.400 top) while the uppermost 220 m have been documented at Glännli (Swiss coordinates: 750.100/222.430 base, 749.990/222.255 top). Correlation is based on a glauconite horizon at 200 m called ‘Chopfbed’ by Briegel (1972) that has been observed in both sections. The transition to the overlying Garschella Formation has been studied in the Sisitz section (Fig. 3).

The Barremian Drusberg beds form a 270 m thick succession of irregularly alternating marl–limestone beds. They consist dominantly of mudstones and wackestones, which contain mainly benthic foraminifera, sponge spicules, calcispheres

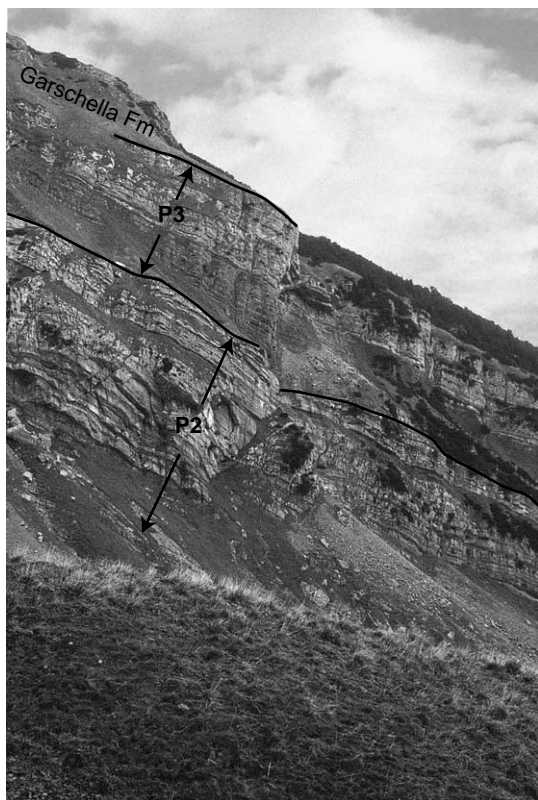


Fig. 2. Photograph of the upper part of the Alvier section (Glaennli) showing the second and third progradation phases of the carbonate platform (P2 and P3) within the Schrattekalk Formation and the overlying Garschella Formation. For scale: thickness of P2 is 160 m.

and echinoderms. In the lowermost 13 m, rare ammonites indicate an age between the *hugii* and the *feraudi* zone (Briegel, 1972). At 200 m, a 5 m thick glauconite-rich horizon has been identified (Briegel, 1972).

The Schrattekalk Formation is characterised by two massively bedded limestone intervals from 270 to 360 m (uppermost Barremian) and from 420 to 440 m (lower Aptian). A marlier interval named ‘Hurstmergel’ separates the limestone successions (Briegel, 1972). Thin sections from the two limestone intervals contain foraminifera, sponge spicules, calcispheres, peloids and abundant reworked and rounded intraclasts, orbitolinids, miliolids, rudist fragments and bryozoans in a micritic matrix (resediments from the nearby platform according to Funk and Briegel, 1979). The composition of the thin-bedded, marly interval is similar to one of the Drusberg beds (Briegel, 1972).

The top of the Schrattekalk Formation studied at Sisitz (Swiss coordinates: 748.250/223.550) contains pockets filled with a micritic, hedbergellid-bearing limestone (Ouweland, 1987). It is overlain by an irregular, several centimetre thick, glauconitic siltstone bed (Luitere bed) containing phosphorite pebbles and abundant clasts (\varnothing ca 1 cm) of a micrite similar to that preserved within the pockets (Fig. 3).

4.1.2. Stable isotope data

All the isotope data are graphically displayed in Fig. 3. The carbon-isotope curve can be split into eight segments (B2–A1 in Fig. 3). Turning points and/or rapid changes in the gradients of the C-isotope curve mark the boundaries between individual segments.

C-isotope values measured at the base of the section (top of lower Barremian) increase from +1.0‰ to values near +2.0‰ (unit B2). An interval of relatively constant $\delta^{13}\text{C}$ values between +1.7‰ and +2.0‰ characterises B3, while B4 shows gradually increasing values reaching a level of +3.0‰. B5 is defined by a decreasing trend towards $\delta^{13}\text{C}$ values near +2.0‰. A renewed increase towards +3.5‰ interrupted by a ‘negative event’ at 250 m characterises B6. Above, from 300 to 330 m, carbon-isotope values fluctuate between

Alvier

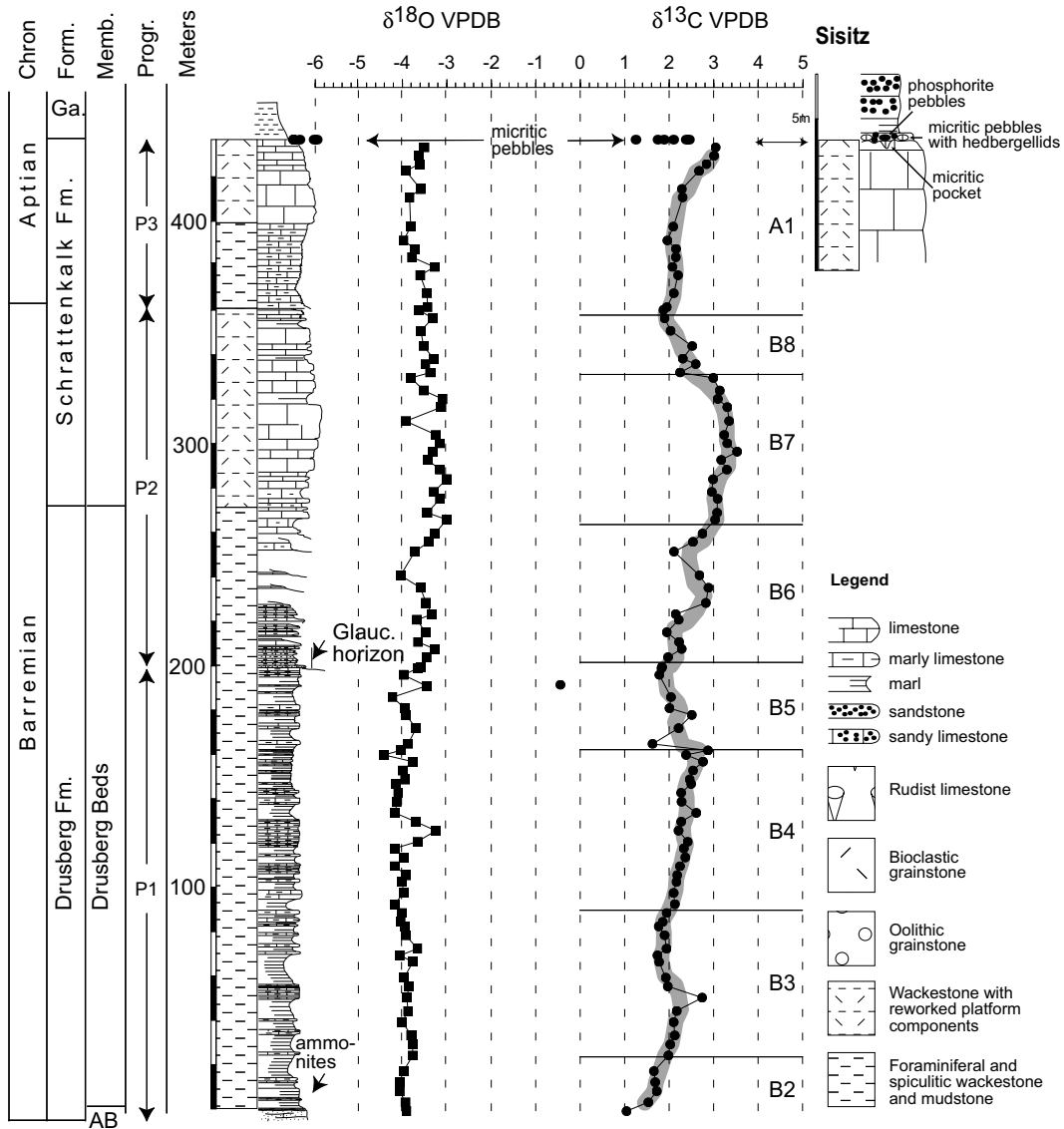


Fig. 3. Alvier sections. The sections have been measured in the field bed by bed. Samples have been taken about every second metre and were investigated using thin sections, peels and polished surfaces. The data for the Riseten/Glaennli profile are from Briegel (1972). See Fig. 4 for the interpretation of the lithofacies. The complete stable isotope data set can be obtained from the third author (H.W.).

+3.0‰ and +3.5‰ (B7). In the following 30 m, at the end of the Barremian, a stepwise decrease to values near +2.0‰ is recorded (B8). In the topmost 80 m of the Alvier section, carbon-isotope values increase again to +3‰ (A1).

The carbon-isotopic composition of the micritic

pebbles on top of the Schrattekalk Formation at Sisitz scatters from +0.6‰ to +2.4‰ (Fig. 3, compare also carbon-isotope measurements in Ouwehand, 1987). The δ¹⁸O of the Alvier section scatters from -4.4‰ to -3.0‰ in the Drusberg and Schrattekalk formations. The micritic peb-

bles on top of the Schrattenkalk Formation have an oxygen isotope composition of -6‰ .

4.2. Churfirften

4.2.1. Sedimentology

In the Churfirften region about 100 m of Drusberg Formation are overlain by the more than 200 m thick Schrattenkalk Formation (Figs. 4 and 5; Heim, 1916). The Drusberg Formation only crops out in the steep flank south of the Churfirften chain and is therefore not accessible, while the Schrattenkalk Formation can be studied in the valleys between the peaks of the Churfirften range (Fig. 4). The N–S striking valleys between the Churfirften mountains reveal up to 2 km long outcrops perpendicular to the palaeoshelf edge and the sheer cliffs on the southern side of the peaks enable observations of the bedding over tens of kilometres approximately parallel to the shelf edge. Sedimentological features indicating channels, slumps or reefs are not observable, and the platform topography appears to have been extremely monotonous.

Most of the Schrattenkalk Formation has been documented within a section along the western flank of the Zuestoll peak (Swiss coordinates: 739.870/224.320 base, 739.950/224.770 top). Additionally, the transition from the bioclastic to the rudist limestone and the top of the Schrattenkalk Formation have been studied in the Chammere valley (Swiss coordinates: 741.900/225.100 and 741.940/225.940, respectively).

The lowermost 80 m of the Schrattenkalk Formation consist of obliquely bedded, coarse, well-sorted grainstones with abundant ooids, intraclasts and well-rounded bioclasts (oolitic limestone). The top of this facies is covered by a 2 m thick package of coral-rich limestone (coral limestone). The following 20 m are characterised by massive, poorly sorted bioclastic grainstone covered by a hardground studied in detail in the Chammere valley (see Fig. 5). The hardground is overlain by a 45 m thick succession of fossil-rich, poorly sorted grainstone and packstone with abundant rudists, nerineids, chaetetids, chondrodonts, miliolids and orbitolinids (rudist limestone). Above, between 165 and 182 m, are finely bedded marly and silty packstones with small ooids (<1 mm), echinoderms and quartz grains. They represent the lithostratigraphic equivalent of the ‘lower Orbitolina Beds’ (Funk et al., 1993). Their age has been determined at a section some kilometres to the north (Säntis) by B. Clavel (written communication). Clavel identified echinids of ‘middle’ Bedoulian age (*consobrinus* zone, which corresponds to the lower *weissi* zone according to Clavel et al., 1995). The topmost 40 m again consist of fossil-rich rudist limestone. About 1 m below the top of the Schrattenkalk Formation a shell of the rudist *Praecaprina* has been identified, indicating an Early Aptian age (Masse, 1998a,b).

The uppermost 15 m of the Schrattenkalk Formation contains sub-vertical cracks filled by glauconitic quartz sand with a micritic matrix (Greber

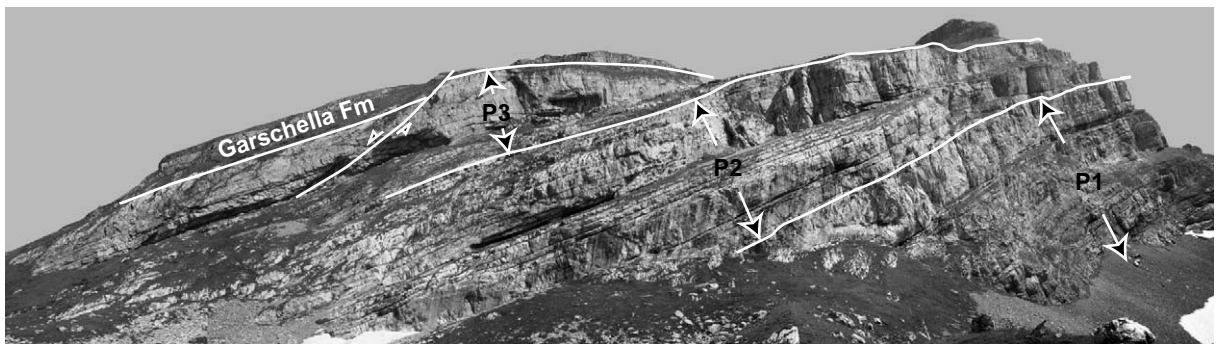


Fig. 4. Photograph of the Zuestoll section (Churfirften) along the western flank of the Zuestoll peak, showing the Schrattenkalk Formation and the overlying Garschella Formation. P1, P2 and P3 are the three progradation phases of the carbonate platform (Schrattenkalk Formation). For scale: thickness of P2 is 60 m.

Zuestoll

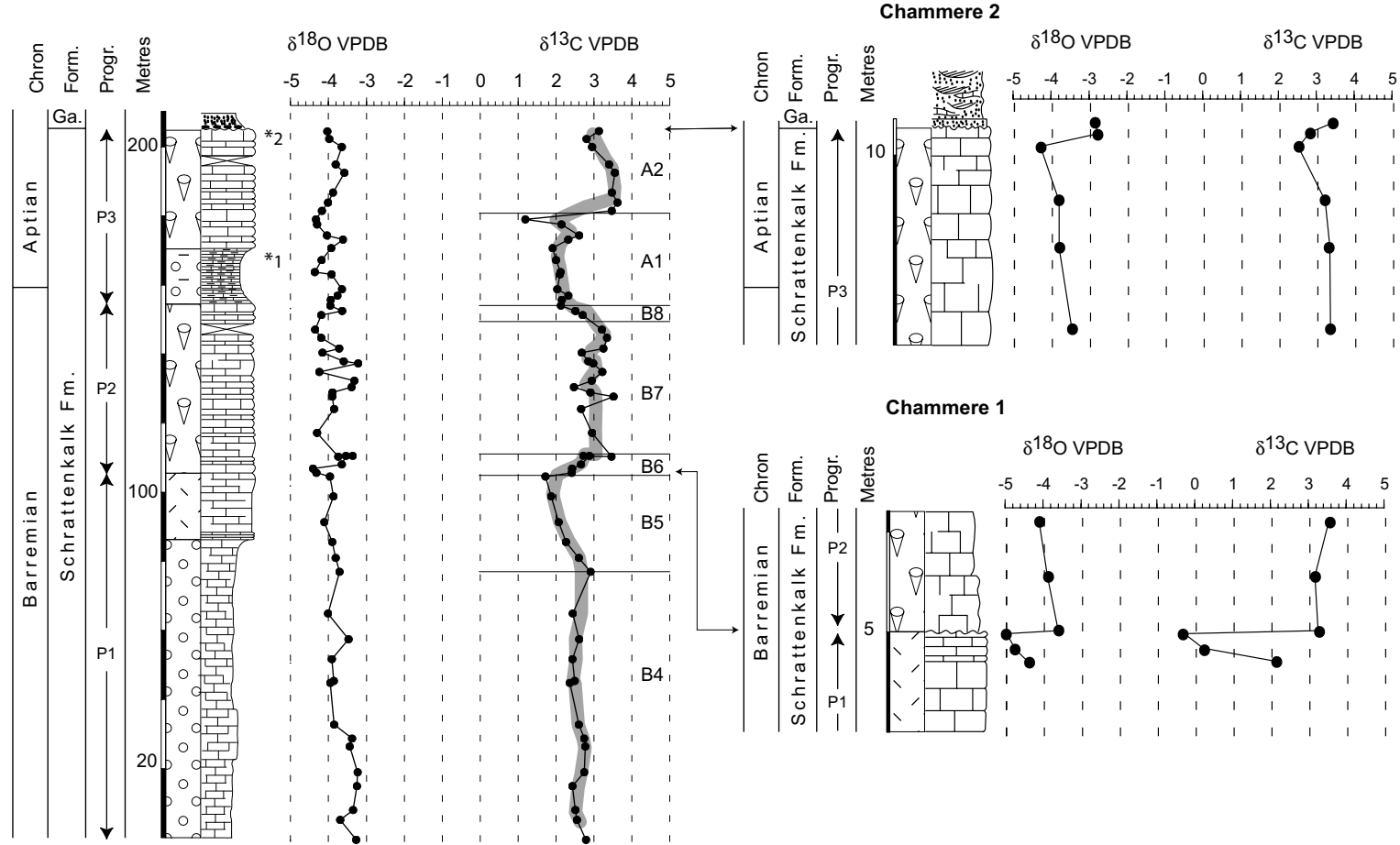


Fig. 5. Churfirten sections. The sections have been measured in the field bed by bed. Samples have been taken about every second metre and were investigated using thin sections, peels and polished surfaces. *1, Dated by echinids as middle Bedoulian (B. Clavel, written communication); *2, dated by Orbitolinids as middle Early Aptian (*Orbitolinopsis buccifer*, *O. briacensis*; Bollinger, 1988, p. 40). See Fig. 4 for the interpretation of the lithofacies and Fig. 2 for the legend. The complete stable data set can be obtained from the third author (H.W.).

and Ouwehand, 1988). Schrattekalk clasts with a diameter of several millimetres and pebbles of partially phosphatised micrites are preserved within the glauconite sandstone. Glauconite sand occurs additionally in pockets and occasionally as fillings of dissolved rudist shells within the top-most bed of the Schrattekalk Formation. Ouwehand (1987) describes bivalve borings on top of the Schrattekalk Formation filled with hedbergellid-bearing micritic limestone. In some places a thin (1 cm) autochthonous phosphoritic crust covers the uppermost Schrattekalk bed (Ouwehand, 1987).

4.2.2. Stable isotope data

All the measured isotope data are graphically displayed in Fig. 5. The carbon-isotope curve can be split into seven segments (B4–A2). Segment B4 shows carbon-isotope values which fluctuate around +2.5‰. Between 80 and 100 m, $\delta^{13}\text{C}$ values decrease and reach compositions of +1.7‰ (B5). B6 is defined by a rapid transition of values near +1.7‰ to compositions around +3.5‰. During B7, carbon-isotope values scatter around +3‰. Above B7, a negative shift of 1‰ within 5 m is recorded (B8). A1 is defined by $\delta^{13}\text{C}$ values close to +2.0‰. The subsequent shift up to +3.5‰ marks the transition into A2, where the curve remains at high values between 2.8‰ and 3.5‰.

In the Zuestoll section, values of the $\delta^{18}\text{O}$ profile vary between -5.5‰ and -3.2‰ . In the lowermost 30 m, within the oolitic limestones, oxygen-isotope values are around -3.2‰ . At 30 m, $\delta^{18}\text{O}$ decreases rapidly within 5 m and remains close to -4.0‰ within the following 80 m of oolitic and bioclastic grainstone. In the overlying rudist limestone and marly limestone, oxygen-isotope values scatter between -4.5‰ and -3.2‰ .

In the Chamhere valley the $\delta^{13}\text{C}$ profile across the hardground at the base of the lower rudist limestone interval displays values as low as -0.3‰ 20 cm below the hardground. A value of +2‰ was measured 150 cm below the hardground. Above the hardground, $\delta^{13}\text{C}$ is around +3.2‰. The $\delta^{13}\text{C}$ record from the uppermost 10 m of the Schrattekalk Formation shows carbon-isotope values of +3.5‰ between 10 and 3 m

below the top of the Schrattekalk Formation. Then, the values decrease to +2.5‰. The oxygen isotope values fluctuate between -5.0‰ and -2.8‰ .

5. Discussion

5.1. Facies interpretation

The monotonous structure of the large-scale outcrops in the Churfirten Mountains suggests that neither reefs nor mounds characterise the palaeotopography of the studied platform. The observed features rather correspond to a homoclinal carbonate ramp with a low slope angle on which shallow and episodically wave- or current-agitated facies of the near-shore zone pass downslope into deeper-water low-energy deposits (Fig. 6; Ahr, 1973; Read, 1985). The facies assemblage fossilised in the Schrattekalk Formation is typical for Early Cretaceous tropical shelf seas and is referred to as the Mesogean benthic ecosystem, which appears to have been the equivalent of modern warm-water carbonate assemblages (Masse, 1992). Based on a detailed facies analysis of the studied carbonate ramp we can classify the studied sediments into four facies types (Figs. 3, 5–7). In the following, we compare the carbonate ramp successions with modern carbonate sediments and we integrate facies types into the carbonate ramp model by Burchette and Wright (1992).

5.1.1. Facies 1: Outer-ramp deposits

Foraminiferal and spiculitic wackestones and mudstones

The foraminiferal and spiculitic wackestones are interpreted as sediments deposited in a water depth below the SWB (stormweather base) on the outer part of the ramp. Small benthic foraminifera and sponges inhabited this environment. The micritic carbonate material was probably delivered from the platform in the north but the marly character of the rocks also indicates continental-influenced sedimentation. Comparable deposits are found today in the eastern Gulf of Mexico (Ginsburg and James, 1974) and on the western

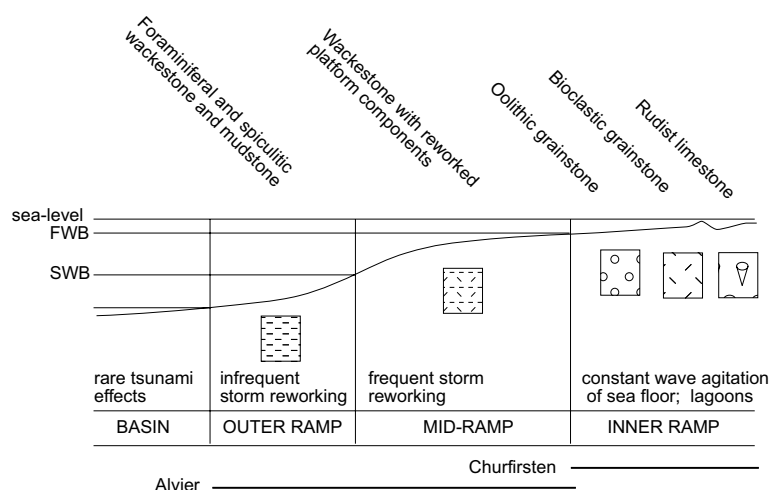


Fig. 6. Carbonate ramp model after Burchette and Wright (1992) and facies distribution of the lithologies found within the Schrattenkalk and Drusberg formations. The legend is the same as in Fig. 2. FWB, fairweather base; SWB, stormweather base.

part of the Yucatan shelf (Logan et al., 1969) in water depths between 30 and 200 m.

5.1.2. Facies 2: Mid-ramp deposits

Wackestone with reworked platform components

We observed rounded lithoclasts and ooids within a micritic matrix. Both rounded lithoclasts and ooids form within a high-energy environment where micritic ooze is winnowed. Therefore, these components are interpreted to have formed on the inner platform and then have been transported into a quiet environment where micritic ooze is preserved. Carbonate sediments with a comparable composition (well-sorted *Halimeda* packstone) are deposited during storm events on off-bank spillover lobes of the South Florida shelf below ca 5 m water depth (Aigner, 1985). According to our interpretation, the wackestones and packstones with reworked platform components (lithoclasts, ooids) of the Schrattenkalk Formation have been deposited in a mid-ramp setting, where from time to time, most probably during storms, bioclastic debris from the high-energy environment was delivered.

5.1.3. Facies 3: Inner-ramp deposits

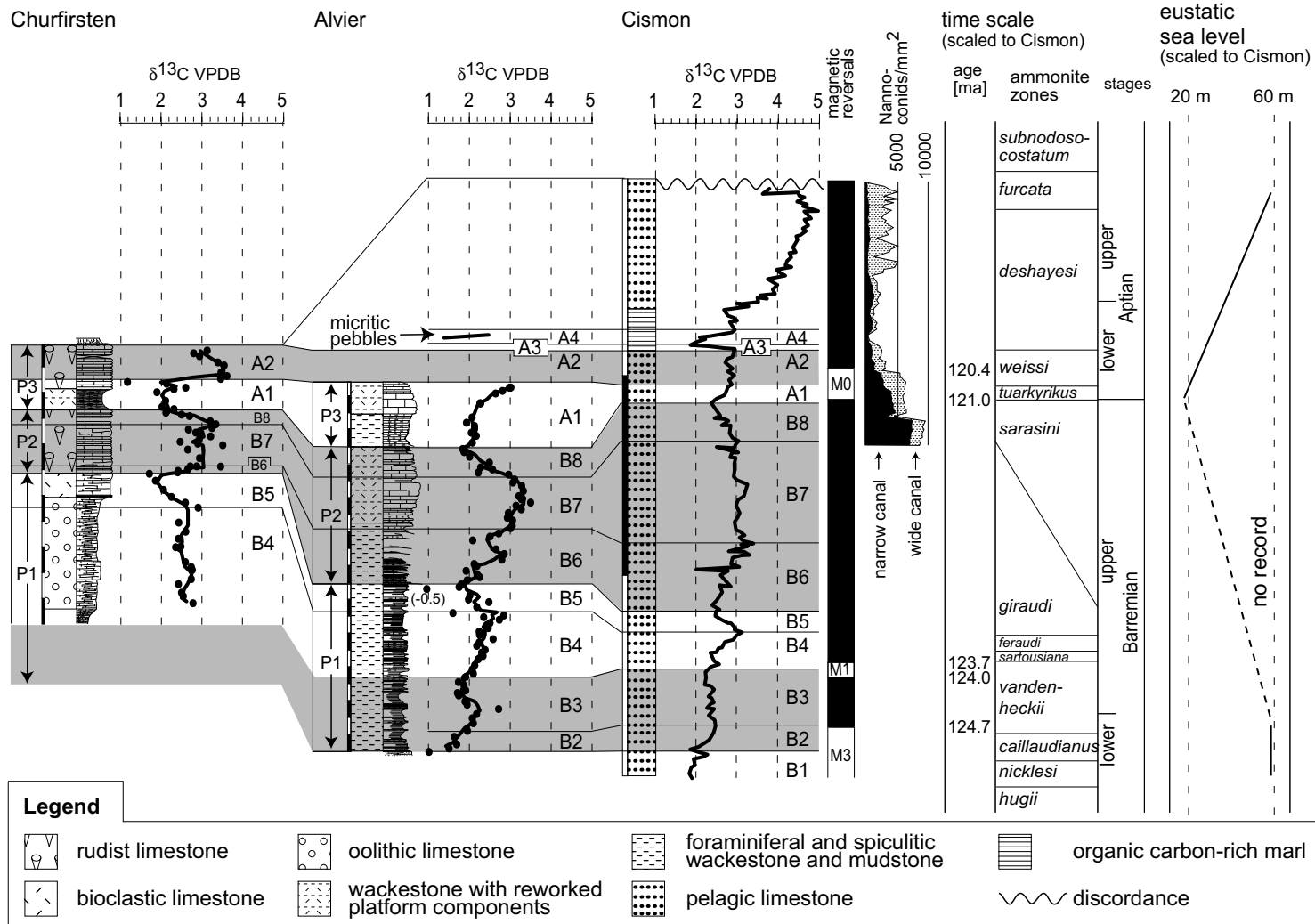
(1) Bioclastic and oolitic grainstones

The well-sorted bioclastic and oolitic grain-

stones represent deposits from a high-energy environment. The massive character of these limestones suggests very high sedimentation rates within the prograding part of the platform, where accommodation space was large. Recent ooids are deposited within tidal deltas of the Arabian Gulf (Purser, 1973), and in shallow water masses agitated by tidal currents and wave energy along leeward platform margins of the Bahama Bank (Newell and Rigby, 1957), as well as within strong, shelf-parallel currents on the inner shelf of northeastern Yucatan (Ward and Brady, 1973). There is no evidence for tidal channels in the sediments of the Schrattenkalk and Drusberg formations. We therefore consider the observed oolite belts to be either of Bahamian or of Yucatan type and to have been deposited within wave- and/or current-agitated water. Moreover, the more proximal low-energy facies described below indicates that wave- and current-energy must have been broken somewhere. Since there are no reefs, the low-energetic lagoonal sediments may have formed behind barriers provided by oolitic bars similar to the carbonate muds on the northeastern Yucatan shelf (Ward and Brady, 1973).

(2) Rudist limestone

The rudist limestones consist of unsorted bioclastic grain- and packstones with large, well-preserved rudist and chondrodont shells, benthic fo-



raminifera such as miliolids, orbitolinids and textularians as well as echinoderms. Most of the bioclasts are strongly micritised. Due to the presence of large shells and the strong micritisation of the bioclasts, these sediments are interpreted as open lagoonal inner-ramp deposits (e.g. Masse, 1976, 1992; Arnaud-Vanneau, 1980). Despite the fact that recent bivalves are much smaller than Early Cretaceous rudists, comparable sediments rich in mollusc shells are common in many shallow-water environments of recent carbonate shelves (Ginsburg and James, 1974) and can be found in water depths less than 100 m, for example, in the Gulf of Mexico (Ginsburg, 1956; Gould and Stewart, 1956; Logan et al., 1969) on the continental shelf off Belize and on the Sahul shelf, as well as on the southern part of the Queensland shelf (Ginsburg and James, 1974).

According to the Burchette and Wright (1992) model the discussed limestone successions correspond to deposits accumulated on the outer, middle and distal inner part of a carbonate ramp. Basinal and intertidal deposits have not been observed. Outer-ramp deposits are represented by foraminiferal and spiculitic wackestone and mudstone, mid-ramp deposits consist of wackestone with storm-reworked platform components and inner-ramp deposits include bioclastic and oolitic grainstone forming shoals in the high-energy, wave-agitated zone, as well as rudist limestone deposited in protected lagoons behind the shoals (Fig. 6). Similar platform models for the sediments of the Schrattekalk and Drusberg formations in other regions of the Helvetic Alps have been presented by Ziegler (1967), Bollinger (1988), Schenk (1992) and Trabold (1996), as well as by

Arnaud-Vanneau (1980) and Masse (1976) for the Urgonian limestone in southeastern France.

5.2. Progradational phases

Within the Drusberg and Schrattekalk formations we have identified three sedimentary cycles (P1, P2 and P3) that reflect three phases of platform progradation separated by transgressions or emersions (Fig. 7). The first progradation event occurs in the Churfirten section and is represented by the transition from the Drusberg Formation into the 120 m thick series of oolitic and bioclastic grainstones of the Schrattekalk Formation (P1). P1 is capped by an exposure horizon (Figs. 5 and 7). At Alvier, the sedimentary cycle P1 comprises a 200 m thick, monotonous succession of outer-platform deposits, demonstrating that shallow-water sediments of the first progradation did not reach far south (Fig. 7). In the Churfirten section, P2 comprises a 45 m thick rudist limestone succession and indicates aggradational sedimentation during this phase of the carbonate ramp deposition. The condensed glauconitic horizon above P1 in the Alvier section documents renewed transgression. We interpret this condensed level as the base of P2. The overlying 160 m record a change from outer- to mid-ramp deposits, indicating renewed progradation of the inner carbonate ramp (Fig. 7). The transition from P2 to P3 is not marked by an emersion horizon. In the Churfirten section, inner carbonate ramp sediments of P2 are replaced by mid-ramp deposits at 165 m and in the Alvier section, outer-ramp sediments overlie mid-ramp deposits. These transitions, marking a renewed transgres-

Fig. 7. Progradational phases recognised in the Churfirten and Alvier regions and correlation of the carbon-isotope profiles from the Helvetic shelf with the Cison profile. P1, P2 and P3 are progradation phases of the Helvetic carbonate platform enabling correlation between Churfirten and Alvier. B1–A4 are elements of the carbon-isotope curve referred to in the text. B2/B3, B6–B8 and A2 are shaded in order to demonstrate clearly the correlated intervals. Isotope curve segments A2–A4 correspond to isotope curve segments C1–C4 in Menegatti et al. (1998, C was written for ‘Cison’). In the Churfirten and Alvier profiles, round spots indicate carbon-isotope measurements, the black line represents a three-point moving average. Lithology, carbon isotopes, magnetic reversals and nannoconid abundance of the Cison section are from Erba et al. (1999) and from Larson and Erba (1999). At the right-hand side we added absolute ages of the magnetic reversals and the Tethyan ammonite zonation that has been correlated with the carbon-isotope curve by Masse et al. (1999) and by Wissler et al. (2002). Since the sedimentation rates of the three sections vary by at least one order of magnitude, the metre scales have been chosen differently in each of the profiles. Each of the black or white elements represents 20 m. The sea-level curve is from Sahagian et al. (1996).

sion, define the base of P3. The last cycle, P3, represents a shallowing upward succession in both sections and mirrors the third progradation phase of the investigated carbonate ramp (Fig. 7).

5.3. Interpretation of the carbon-isotope measurements

5.3.1. Imprint of burial diagenesis on stable isotope composition

The bulk of the measured carbon-isotope values lies between +1‰ and +3.5‰ and corresponds to biogenic calcite precipitated under open marine conditions during the Barremian and Aptian (Weissert, 1989; Menegatti et al., 1998; Erba et al., 1999), whereas all $\delta^{18}\text{O}$ values scatter between -6‰ and -3.5‰ and are depleted by 3‰ or more relative to diagenetically unaltered marine calcite (Clarke and Jenkyns, 1999). Our data suggest that the oxygen-isotope composition of the measured samples reflects elevated temperature during burial diagenesis and incipient recrystallisation during orogeny, while the carbon-isotopic composition has been less affected by these processes (e.g. Weissert, 1989).

Limestone samples from the vicinity of exposure surfaces are often depleted in ^{13}C and ^{18}O due to cementation under meteoric conditions and palaeosol formation. Burial diagenesis and incipient metamorphism led to re-equilibration of the oxygen-isotope signature. Therefore we cannot use $\delta^{18}\text{O}$ compositions of the limestones analysed as a fingerprint of meteoric diagenesis. In contrast, the $\delta^{13}\text{C}$ values could still preserve an original meteoric signature (James and Choquette, 1990; Wagner, 1990; Fouke et al., 1995; Chafetz and Rush, 1995). The ^{13}C -depleted samples measured below the top of progradation cycle P1 (Chammere section; Fig. 3) can therefore be interpreted as indicators of cementation under meteoric conditions during the sea-level lowstand, which marks the boundary between P1 and P2.

On modern carbonate platforms, water in restricted environments becomes enriched in light carbon from respiration, freshwater discharge and CaCO_3 withdrawal (Lazar and Erez, 1990; Patterson and Walter, 1994). Facies poorly affected by these processes are outer- and mid-plat-

form deposits as well as distal inner-platform sediments such as oolitic belts. The influence becomes stronger towards lagoonal and intertidal realms (Patterson and Walter, 1994) and within marine brines (Lazar and Erez, 1990). In the studied successions rudist limestones were deposited in the most proximal carbonate environment. This may explain the larger scatter of the carbon-isotope data within the lagoonal rudist limestone compared to the measurements in the more distal facies belts. The outstanding and extremely depleted carbon-isotope value (-0.5‰) measured at 195 m of the Alvier section cannot be related to an emersion event. It may either record an original negative carbon-isotope anomaly of Tethyan seawater or it could have been the result of locally restricted conditions also resulting in ^{13}C depletion of coastal waters.

The main pattern of the measured C-isotope signal, as expressed by the three-point moving average, neither features restricted oceanographic conditions nor indicates alteration during diagenesis. The trends of the two carbon-isotope curves established in the two carbonate ramp sections show the same pattern and absolute values are also comparable. Also, the shallowing-upward trends in both profiles are not accompanied by a decrease in $\delta^{13}\text{C}$. Thus, we assume that the measured carbon-isotope values reflect changes in the isotopic composition of the global oceanic carbon reservoir, and that we can use the $\delta^{13}\text{C}$ curves for correlation.

5.3.2. Carbon-isotope stratigraphy

Based on our carbon-isotope analyses and on available biostratigraphic information we propose a platform-basin correlation as presented in Fig. 7. In a first step, we use ammonite stratigraphy for correlation of the base of the Alvier profile with the Cismon profile. Ammonites found within the Altmann bed at the base of the Drusberg Formation indicate that condensation began during the *angulicostata* zone and continued until the *caillaudianus* zone (Funk et al., 1993), while ammonites from the lowermost 13 m of the Drusberg beds suggest an age between the *hugii* and the *feraudi* zone (Briegel, 1972). Thus, the base of the carbon-isotope profile is not older than the

caillaudianus and not younger than the *ferraudi* zone. A carbon-isotope profile from the Vocontian trough shows that the transition from the *caillaudianus* to the *vandenheckeii* zone is marked by a $\delta^{13}\text{C}$ increase of 0.5‰, which correlates with the late Early Barremian increase in B2 at Cismon (Wissler et al., 2002). Therefore, the positive carbon-isotope shift within the lowermost 20 m of the Alvier section corresponds to the B2 increase at Cismon marking the transition from magnetozone M3 to M2. Isotope intervals described here as B3–B8 can be identified in both the Cismon profile and in the carbonate ramp limestones. The carbon-isotope curve in the carbonate ramp record shows fluctuations with a larger amplitude than observed in the pelagic C-isotope curve. This is in agreement with observations made in earlier C-isotope investigations of shallow-water environments (e.g. Jenkyns, 1995; Vahrenkamp, 1996). It may indicate that shallow-water settings are less stable in their isotopic composition and that a variety of factors, including changes in productivity, may amplify changes of the global oceanic carbon reservoir.

We correlate the rising carbon-isotope values in A1 near the top of the Alvier section with the earliest Aptian increase within M0 at Cismon. The interval A2 occurs only in the Churfirsten section but not in the Alvier section. This may be due either to changes in the local current and sediment distribution pattern during this interval or it may indicate a first back-stepping of the platform due to decreasing carbonate production in the shallower ramp environment.

The phosphoritic horizon covering the top of the Schratteknalk Formation contains ammonites of the *crassicostatum* to *melchioris* zones (Ouweland, 1987). Hence, the reworked pelagic limestone pebbles found within the Luitere bed are older than the *crassicostatum* zone but younger than A2. Their isotopic composition varies between 0.6‰ and 2.4‰. The only time when values of this range are recorded in alpine pelagic limestones after A2 and before or during the *crassicostatum* zone is within the negative carbon-isotope spike (A3/A4) at the beginning of the deposition of the Livello Selli (Bralower et al., 1999; Groecke et al., 1999; Menegatti et al., 1998). The

scatter from 0.6‰ to 2.4‰ within the different pebbles suggests that they represent remnants of sediments deposited during the rapid decrease and/or increase of oceanic $\delta^{13}\text{C}$ value.

Based on our investigations we conclude that the growth crisis and the subsequent drowning of the studied carbonate platform occurred within a time window starting in A1 and peaking immediately before the A3 negative carbon-isotope shift. The observed carbonate platform growth crisis coincided with a major biocalcification crisis in pelagic environments. Erba (1994) recognised a first decrease in the abundance of wide and narrow channel nannoconids within carbon-isotope interval B8. This decrease coincides with the top of progradation cycle P2 and with the following transgression of A1, a time of incipient platform growth crisis, which, in our area of study, only affected the more distal carbonate ramp environment (locality Alvier). The most dramatic collapse of the Tethyan nannoconid assemblage occurred during A2 and A3 when the thick-shelled calcareous nannofossils disappeared from many pelagic sediments for about 1 Myr.

Carbon-isotope profiles are also available for the central (Angle) and marginal (La Bédoule) regions of the Vocontian basin (Wissler et al., 2002; Kuhnt et al., 1998), as well as for the Provence platform (Mont Vacluse; Masse et al., 1999). A first drowning episode at the very end of the Barremian resulted in the disappearance of the Urgonian platform (B8–A1). Stepwise drowning of the Provence platform culminated at the transition *weissi–deshayesi* zone and it is recorded in an abrupt lithological change from bioclastic limestones to marls (Masse, 1998a,b). This transition also coincides with the onset of the Early Aptian negative carbon-isotope event at both sites from the Vocontian basin. This lithological change is also correlated with the top of the Vercors carbonate platform (Arnaud et al., 1998). These data suggest that a stepwise collapse of carbonate platforms starting in the latest Barremian and peaking during isotope segment A3 was not limited to the Helvetic margin but that it affected wide areas of the northern Tethys carbonate coast. Only in some areas of the Provence region, most of the Aptian positive carbon-isotope shift

seems preserved in carbonate platform sediments (Masse et al., 1999), and the carbonate platform sedimentation appears to continue up to the Late Aptian similar to southern Tethyan carbonate platforms (Ferreri et al., 1997).

5.4. Drowning and carbonate crisis

The top of the Schrätkalk Formation has experienced a complex history of sedimentation and erosion phases. Despite intensive research based on petrographic and cathodoluminescence observations, it was so far impossible to detect any features related to meteoric diagenesis within the uppermost beds of the Schrätkalk Formation of eastern Switzerland (Ouwehand, 1987; Bollinger, 1988). Since the carbon isotopes also do not show a pronounced negative trend indicating early meteoric cementation (Fig. 3), it is likely that the platform drowned without preceding exposure. The oldest post-drowning sediment found is the micritic limestone preserved within erosional pockets and borings on top of the Schrätkalk Formation, and as pebbles within the Lutere bed, as well as within the glauconitic sands infilling the cracks in the top of the Schrätkalk Formation. The hedbergellid-bearing micrite documents a deepening of the environment and a phase of low continental siliciclastic sediment input (Ouwehand, 1987; Bollinger, 1988). It was originally deposited on top of the Schrätkalk Formation and most probably reworked and partially phosphatised during the development of the autochthonous phosphorite crust on top of the Schrätkalk Formation when strong currents polished the shelf (Ouwehand, 1987). The glauconitic sandstone within the cracks in the top of the Schrätkalk Formation is younger than the autochthonous phosphorite crust and the micritic limestone because it contains reworked pebbles of both lithologies. The fractures in the top of the Schrätkalk Formation do not reveal any dissolution or erosion features and result from tectonic stress, as indicated by their geometric relationship (Greber and Ouwehand, 1988).

The Early Aptian drowning of the carbonate platform in eastern Switzerland occurred during a time of globally rising sea level (Jacquin et al.,

1998; Sahagian et al., 1996). On the Russian platform, an Early Aptian sea-level rise of 40 m within a time of 4 Myr has been recorded (Sahagian et al., 1996). The subsidence rate on the Helvetic shelf north of our study area was 15 m/Myr and in the Alvier region 50 m/Myr (Funk, 1985). The combination of eustatic sea-level rise and subsidence produced an increase in accommodation space of 25 m/Myr in the north and 65 m/Myr in the south. This is, at least in the north, less than the lowest accumulation rates for prograding carbonates (30 m/Myr) cited by Schlager (1981) and 10 times less than accumulation rates calculated for platforms in the Dolomites (Schlager, 1981). Thus, under environmental conditions favourable for carbonate-precipitating organisms, the Helvetic carbonate ramp should have been able to compensate for Early Aptian relative sea-level rise (Schlager, 1981).

Factors weakening the growth potential of carbonate platforms are cool seawater temperatures (e.g. Isern et al., 1996), elevated nutrient concentrations (Hallock and Schlager, 1986; Masse and Montaggioni, 2001) and rising atmospheric pCO₂ (Gattuso et al., 1998). The contemporaneously occurring drowning on the wide parts of the northern Tethyan shelf and the ‘nannoconid decline’ in the open ocean (Erba, 1994) suggest that calcification rates in selected pelagic and neritic organisms were weakened in both pelagic and platform environments during the Barremian–Aptian transition. According to Larson and Erba (1999) the Late Barremian and Early Aptian was a time of strongly enhanced volcanic activity and thus probably also a time of rising atmospheric pCO₂ (Bernier, 1991). The observed Tethyan biocalcification crisis starts at the time of peak volcanic activity on the Ontong–Java Plateau, dated as 119–125 Myr (Tejada et al., 2002). The crisis culminates at the beginning of the prominent negative carbon-isotope spike A3 (Menegatti et al., 1998). The negative carbon-isotope spike is believed to be the result of a sudden climate-induced release of methane from the sediments into the ocean/atmosphere. The oxidation of ¹³C-depleted methane (Hesselbo et al., 2000; Weissert, 2000; Jahren et al., 2001) would have resulted in an additional flux of CO₂ into the at-

mosphere (Dickens, 2000; Jahren et al., 2001). Data from stomatal indices of fossil Ginkgo leaves support isotope-based $p\text{CO}_2$ reconstructions. They indicate a pronounced rise of atmospheric $p\text{CO}_2$ during the Early Aptian (Retallack, 2001). So far the impact of rising $p\text{CO}_2$ was believed to trigger the Early Aptian carbonate crisis only indirectly. Weissert (1989), Erba (1994) and Föllmi et al. (1994) suggested that accelerated chemical weathering due to globally warmer temperatures resulted in increased nutrient mobilisation and in eutrophication of seawater. Masse and Montagnoni (2001) emphasise the importance of oceanic nutrient flux for primary production in shallow-marine carbonate settings. They propose that changes in coastal upwelling could have triggered the observed biocalcification crisis on platforms. A problem not yet considered for the development of Early Cretaceous carbonate platforms and nannoplankton is that rising $p\text{CO}_2$ affects not only atmospheric temperature but also ocean chemistry. Adding CO_2 to the atmosphere and ocean decreases pH and carbonate-ion concentration of surface waters and thus lowers the calcium carbonate oversaturation. In the context of the recent anthropogenically induced rise of atmospheric $p\text{CO}_2$, the degree of oversaturation has been shown to be an important parameter controlling the growth potential of calcium carbonate precipitating organisms. Experiments with corals, green algae and calcareous nannoplankton demonstrate that a decrease in oversaturation weakens the calcification potential of organisms (Gattuso et al., 1998; Kleypas et al., 1999; Gattuso and Buddemeier, 2000; Riebesell et al., 2000). Lowered oversaturation due to rising $p\text{CO}_2$ could explain the widespread nature of the Early Aptian carbonate platform crisis. It could also explain the seemingly synchronous nannoconid crisis. Changes in nutrient availability related to changes in upwelling intensity and variations in temperature may have been important as local or regional stress-amplifying factors. The Barremian to Early Aptian carbonate platforms growing along the Helvetic shelf, close to exposed land area, were subjected to nutrient and suspension supply from weathering and they may have reacted very sensitively to $p\text{CO}_2$ fluctuations. In contrast,

the carbonate platforms on the Adriatic microplate were not affected by continental influence and they did not drown to the same extent during the Early Aptian $p\text{CO}_2$ rise (D'Argenio et al., 1993). In addition, elevated production rates of oceanic basalts during the mid-Cretaceous should have altered the Mg/Ca ratio of the seawater. Extremely low Mg/Ca ratios during the middle Cretaceous could have contributed to low aragonite saturation and to an observed major change in composition of skeletal particles occurring during the late Early Aptian (see Steuber, 2002).

The addition of high quantities of CO_2 to the ocean–atmosphere system should also have caused a shallowing of the calcite compensation depth. Indeed, Menegatti et al. (1998) have documented how the negative carbon-isotope anomaly at the base of the Livello Selli coincides with a remarkable drop in carbonate content. An even more pronounced drop in carbonate content is recognised in the Appennines, where the Livello Selli was first described by Coccioni et al. (1987). There, the base of the Livello Selli, which corresponds to the base of the ‘green level’, is defined by the transition from a pelagic limestone to marls and carbonate-free claystones. Carbonate contents remained low throughout the Livello Selli in the Appennine sections. The drop in carbonate content observed in Tethyan pelagic sediments could be construed as evidence for accelerated carbonate dissolution triggered by a sudden methane-derived increase in carbon dioxide.

6. Conclusions

In this study we investigated whether the Early Aptian carbonate-platform growth crises were related to the pronounced Early Aptian disturbances of the exogenic carbon cycle. As an area of study we chose a segment of the northern Tethyan carbonate ramp today outcropping in the Helvetic Alps of Switzerland. We could correlate the $\delta^{13}\text{C}$ record from the studied platform with the C-isotope curve in a pelagic succession in the Southern Alps (Cismon section, Northern Italy) and with other carbon-isotope curves covering the Barremian–Aptian transition. The correlation indicates

that the platform drowning on the Helvetic shelf has the same age as platform collapse in other parts of the northern Tethys and that it coincides with the ‘nannoconid crisis’ documented in pelagic sediments by Erba (1994). Decreased calcium carbonate oversaturation during a time of rising pCO₂ due to enhanced volcanic activity possibly amplified by additional methane release best explains the contemporaneous biocalcification crisis recorded in shallow and open oceanic settings. Similar to predictions for modern reefs, the Cretaceous platforms reacted more sensitively to rising pCO₂ when they were exposed to additional environmental stress factors such as elevated nutrient supply or cool water temperature.

Acknowledgements

We thank U. Gerber for photographic help, U. Briegel for his introduction into the field geology of the Alvier region and M. Andres for her comments on an earlier version of this manuscript. S. Bernasconi provided most important help in our stable isotope laboratory. We thank J.P. Masse and T. Steuber for their helpful reviews. Financial support from the Swiss Science Foundation Project 20-53682-98 is gratefully acknowledged.

References

- Ahr, W.M., 1973. The carbonate ramp: an alternative to the shelf model. *Gulf Coast Assoc. Geol. Soc.* 23, 221–225.
- Aigner, T., 1985. Storm depositional systems. *Lecture Notes in Earth Sciences*. Springer, Berlin, 174 pp.
- Alsharan, A.S., Nairn, A.E., 1993. Carbonate platform models of Arabian Cretaceous reservoirs. In: Simo, T., Scott, R.W., Masse, J.-P. (Eds.), *Cretaceous Carbonate Platforms*. AAPG Mem. 56, 173–184.
- Arnaud, H., Arnaud-Vanneau, A., Delanoy, G., 1998. Répartition des Orbitolinidés de la plate-forme Urgonienne (SE de la France). *Géol. Alp.* 74, 4–75.
- Arnaud-Vanneau, A., 1980. Micropaléontologie, paléocéologie et sédimentologie d’une plateforme-carbonatée de la marge passive de la Téthys: L’Urgonien du Vercors septentrional et de la Chartreuse (Alpes occidentales). *Mém. Géol. Alp.* 11, 874 pp.
- Arnaud-Vanneau, A., Arnaud, H., 1990. Hauterivian to Lower Aptian carbonate shelf sedimentation and sequence stratigraphy in the Jura and northern Subalpine chains (southeastern France and Swiss Jura). In: Tucker, M.E., Wilson, J.L., Crevello, P.D., Sarg, J.F., Read, J.F. (Eds.), *Carbonate Platforms, Facies, Sequences, and Evolution*. IAS Spec. Publ. 9, 203–234.
- Berner, R.A., 1991. A model for atmospheric CO₂ over Phanerozoic time. *Am. J. Sci.* 291, 339–376.
- Bollinger, D., 1988. Die Entwicklung des distalen osthelvetischen Schelfes im Barremian und Früh-Aptian. Ph.D. Thesis, Univ. Zürich, 124 pp.
- Bosellini, A., Morsilli, M., Neri, C., 1999. Long-term event stratigraphy of the Apulia platform margin (upper Jurassic to Eocene, Gargano, southern Italy). *J. Sediment. Res.* 69, 1241–1252.
- Bralower, T.J., CoBabe, E., Clement, B., Sliter, W.V., Osburn, C.L., Longoria, J., 1999. The record of global change in Mid-Cretaceous (Barremian-Albian) sections from the Sierra Madre, northeastern Mexico. *J. Foram. Res.* 29, 418–437.
- Briegel, U., 1972. Geologie der östlichen Alviergruppe unter besonderer Berücksichtigung der Drusberg- und Schrattekalkformation. *Eclogae Geol. Helv.* 65, 425–483.
- Burchette, T.P., Wright, V.P., 1992. Carbonate ramp depositional systems. *Sediment. Geol.* 79, 3–57.
- Chafetz, H.S., Rush, P.F., 1995. Two-phase diagenesis of quaternary carbonates, Arabian Gulf: insights from $\delta^{13}\text{C}$ and $\delta^{18}\text{C}$ data. *J. Sediment. Res. A* 65, 294–305.
- Clarke, L.J., Jenkyns, H.C., 1999. New oxygen isotope evidence for long-term Cretaceous climatic change in the Southern Hemisphere. *Geology* 27, 699–702.
- Clavel, B., Charrolais, J., Schroeder, R., Busnardo, R., 1995. Réflexions sur la biostratigraphie du Crétacé inférieur et sur sa complémentarité avec l’analyse séquentielle: exemple de l’Urgonien jurassien et subalpin. *Bull. Soc. Géol. France* 166, 663–680.
- Coccioni, R., Nesci, O., Tramontana, M., Wezel, F.C., Morretti, E., 1987. Descrizione di un Livello-Guida ‘Radiolaritico-Bituminoso-Ittiolitico’ alla base delle marne a Fucoidi nell’ Appennino Umbro-Marchigiano. *Bull. Soc. Geol. Ital.* 183–192.
- D’Argenio, B., Ferreri, V., Ardillo, F., Buonocunto, F.P., 1993. Microstratigrafia e stratigrafia sequenziale. Studi sui depositi di piattaforma carbonatica nel Cretaceo del Monte Maggiore (Appennino Meridionale). *Boll. Soc. Geol. Ital.* 112, 739–749.
- Dickens, G.R., 2000. Methane oxidation during the late Palaeocene thermal maximum. *Bull. Soc. Geol. France* 171, 37–49.
- Erba, E., 1994. Nannofossils and superplumes: The Early Aptian ‘nannoconid crisis’. *Paleoceanography* 9, 483–501.
- Erba, E., Channell, J., Claps, M., Larson, R., Opdyke, B., Premoli-Silva, I., Riva, A., Salvini, G., Torricelli, S., 1999. Integrated stratigraphy of the Cismon APTICORE (Southern Alps, Italy): A ‘reference section’ for the Barremian-Aptian interval at low latitudes. *J. Foram. Res.* 29, 371–391.
- Erba, E., Larson, R.L., 1998. The Cismon APTICORE (south-

- ern Alps, Italy): 'Reference section' for the Lower Cretaceous at low latitudes. *Riv. Ital. Paleontol. Stratigr.* 104, 181–192.
- Ferreri, V., Weissert, H., d'Argenio, B., Buonocunto, F.P., 1997. Carbon isotope stratigraphy: a tool for basin to platform correlation. *Terra Nova* 9, 57–61.
- Föllmi, K.B., Weissert, H., Bisping, M., Funk, H., 1994. Phosphogenesis, carbon-isotope stratigraphy and carbonate platform evolution along the northern Tethyan margin. *Geol. Soc. Am. Bull.* 106, 729–746.
- Fouke, B.W., Everts, A.J., Zwart, E.W., Schlager, W., Smalley, P.C., Weissert, H., 1995. Subaerial exposure unconformities on the Vercors carbonate platform (SE France) and their sequence stratigraphic significance. In: Howell, J.A., Aitken, J.F. (Eds.), *High Resolution Sequence Stratigraphy: Innovations and Applications*. *Geol. Soc. London Spec. Publ.* 104, 295–320.
- Funk, H., 1985. Mesozoische Subsidenzgeschichte im helvetischen Schelf der Ostschweiz. *Eclogae Geol. Helv.* 78, 249–272.
- Funk, H., Briegel, U., 1979. Le faciès Urgonien des nappes Helvétiques en Suisse orientale. *Mém. Spéc. Géobios* 3, 159–168.
- Funk, H., Föllmi, K.B., Mohr, H., 1993. Evolution of the Tithonian-Aptian carbonate platform along the northern Tethyan margin, Eastern Helvetic Alps. In: Simo, T., Scott, R.W., Masse, J.-P. (Eds.), *Cretaceous Carbonate Platforms*. *AAPG Mem.* 56, 387–409.
- Gattuso, J.P., Buddemeier, R.W., 2000. Ocean biogeochemistry; calcification and CO₂. *Nature* 407, 311–313.
- Gattuso, J.-P., Frankignoulle, M., Bourge, I., Romaine, S., Buddemeier, R.W., 1998. Effect of calcium carbonate saturation of seawater on coral calcification. *Glob. Planet. Change* 18, 37–46.
- Ginsburg, R.N., 1956. Environmental relationships of grain size and constituent particles in some South Florida carbonate sediments. *AAPG Bull.* 40, 2384–2427.
- Ginsburg, R.N., James, N.P., 1974. Holocene carbonate sediments of continental shelves. In: *The Geology of Continental Margins*. Springer, Berlin, pp. 137–155.
- Gould, H.R., Stewart, R.H., 1956. Continental terrace sediments in the northeastern Gulf of Mexico. In: *Finding Ancient Shorelines*. *SEPM Spec. Publ.* 3, 2–19.
- Greber, E.A., Ouwehand, P.J., 1988. Spaltenfüllungen im Dach der Schratzenkalk-Formation. *Eclogae Geol. Helv.* 81, 373–386.
- Groecke, D.R., Hesselbo, S.P., Jenkyns, H.C., 1999. Carbon-isotope composition of Lower Cretaceous fossil wood; ocean-atmosphere chemistry and relation to sea-level change. *Geology* 27, 155–158.
- Groecke, D., 2002. The carbon isotope composition of ancient CO₂ based on higher-plant organic matter. *Philos. Trans. R. Soc. Lond. A* 360, 633–658.
- Grötsch, J., Billing, I., Vahrenkamp, V., 1998. Carbon-isotope stratigraphy in shallow water carbonates: implications for Cretaceous black shale deposition. *Sedimentology* 45, 623–634.
- Hallock, P., Schlager, W., 1986. Nutrient excess and the demise of coral reefs and carbonate platforms. *Palaios* 1, 389–398.
- Heim, A., 1916. *Monographie der Churfürsten Mattstock-Gruppe*. In: *Beitraege zur Geologischen Karte der Schweiz, Neue Folge* 20, 573 pp.
- Hesselbo, S.P., Groecke, D.R., Jenkyns, H.C., Bjerrum, C.J., Farrimond, P., Morgans-Bell, H.S., Green, O.R., 2000. Massive dissociation of gas hydrate during a Jurassic oceanic anoxic event. *Nature* 406, 392–395.
- Hunt, D., Tucker, M.E., 1993. The Middle Cretaceous Urgonian platform of Southeastern France. In: Simo, T., Scott, R.W., Masse, J.-P. (Eds.), *Cretaceous Carbonate Platforms*. *AAPG Mem.* 56, 409–453.
- Isern, A.R., McKenzie, J.A., Feary, D.A., 1996. The role of sea-surface temperature as a control on carbonate platform development in the western Coral Sea. *Palaeogeogr. Palaeoclimatol. Palaeoecol.* 124, 247–272.
- Jacquín, T., Rusciadelli, G., Amedro, F., Graciansky, P., Magniez-Jannin, F., 1998. The north Atlantic cycle: An overview of 2nd-order transgressive/regressive facies cycles in the lower Cretaceous of western Europe. In: Graciansky, P., Hardenbol, J., Jacquín, T., Vail, P.R. (Eds.), *Mesozoic and Cenozoic Sequence Stratigraphy of European Basins*. *SEPM Spec. Publ.* 60, 397–409.
- Jahren, A.H., Arens, N.C., Sarmiento, G., Guerrero, J., Amundson, R., 2001. Terrestrial record of methane hydrate dissociation in the Early Cretaceous. *Geology* 29, 159–162.
- James, N.P., Choquette, P.W., 1990. Limestones - The meteoric diagenetic environment. In: McIlreath, A., Morrow, D.W. (Eds.), *Diagenesis*. *Geoscience Canada Reprint Series* 4, 35–73.
- Jansa, L.F., 1993. Early Cretaceous carbonate platforms of the Northeastern North American margin. *Cretaceous Carbonate Platforms*. In: Simo, T., Scott, R.W., Masse, J.-P. (Eds.), *Cretaceous Carbonate Platforms*. *AAPG Mem.* 56, 111–126.
- Jenkyns, H.C., 1995. Carbon-isotope stratigraphy and palaeoceanographic significance of the lower Cretaceous shallow water carbonates of Resolution Guyot, Mid-Pacific mountains. *Proc. ODP Sci. Results* 143, 99–104.
- Jenkyns, H.C., Wilson, P.A., 1999. Stratigraphy, paleoceanography, and evolution of Cretaceous Pacific guyots; relics from a greenhouse Earth. *Am. J. Sci.* 299, 341–392.
- Kleypas, J.A., Buddemeier, R.W., Archer, D., Gattuso, J.-P., Langdon, C., Opdyke, B.N., 1999. Geochemical consequences of increased atmospheric carbon dioxide on coral reefs. *Science* 284, 118–119.
- Kuhnt, W., Moullade, M., Masse, J.-P., Erlenkeuser, H., 1998. Carbon-isotope stratigraphy of the lower Aptian historical stratotype at Cassis-La Bédoule (SE France). *Géol. Méd.* 3/4, 63–79.
- Larson, R.L., Erba, E., 1999. Onset of the mid-Cretaceous greenhouse in the Barremian-Aptian: Igneous events and the biological, sedimentary, and geochemical responses. *Palaeoceanography* 14, 663–678.
- Lazar, B., Erez, J., 1990. Extreme ¹³C depletions in seawater-

- derived brines and their implications for the past geochemical carbon cycle. *Geology* 18, 1191–1194.
- Lehman, C., Osleger, D.A., Montañez, I.P., 1998. Controls on cyclostratigraphy of Lower Cretaceous carbonates and evaporites, Cupido and Coahuila platforms, Northeastern Mexico. *J. Sediment. Res.* 68, 1109–1130.
- Logan, B.W., Harding, J.L., Ahr, W.M., Williams, J.D., Snead, R.G., 1969. Late Quaternary carbonate sediments of Yucatan shelf, Mexico. In: *Carbonate Sediments and Reefs, Yucatan Shelf, Mexico*. AAPG Mem. 11, 1–128.
- Masse, J.-P., 1976. Les calcaires urgoniens de Provence. Dissertation, Univ. Marseille, 445 pp.
- Masse, J.-P., 1992. The Lower Cretaceous Mesogean benthic ecosystems: palaeoecologic aspects and palaeobiogeographic implications. *Palaeogeogr. Palaeoclimatol. Palaeoecol.* 91, 331–345.
- Masse, J.-P., 1993. Valanginian-Early Aptian carbonate platforms from Provence, southeastern France. In: Simo, T., Scott, R.W., Masse, J.-P. (Eds.), *Cretaceous Carbonate Platforms*. AAPG Mem. 56, 363–374.
- Masse, J.-P., 1998. Rudists. In: Graciansky, P., Hardenbol, J., Jacquin, T., Vail, P.R. (Eds.), *Mesozoic and Cenozoic Sequence Stratigraphy of European Basins*. SEPM Spec. Publ. 60, 775.
- Masse, J.P., 1998b. Sédimentologie du stratotype historique de l'Aptien inférieur dans la région de Cassis-La Bedoule (S.E. France). *Géol. Méd.* 3/4, 31–41.
- Masse, J.P., El Albani, A., Erlenkeuser, H., 1999. Stratigraphie isotopique ($\delta^{13}\text{C}$) de l' Aptien inférieur de Provence (SE France): Application aux corrélations plate-forme/bassin. *Eclogae Geol. Helv.* 92, 259–263.
- Masse, J.P., Montaggioni, L.F., 2001. Growth history of shallow-water carbonates: control of accommodation on ecological and depositional processes. *Int. J. Earth Sci.* 90, 452–469.
- Menegatti, A.P., Weissert, H., Brown, R.S., Tyson, R.V., Farimond, P., Strasser, A., Caron, M., 1998. High-resolution $\delta^{13}\text{C}$ stratigraphy through the Early Aptian 'Livello Selli' of the Alpine Tethys. *Paleoceanography* 13, 530–545.
- Newell, N.D., Rigby, J.K., 1957. Geological studies on the Great Bahama Bank. *SEPM Spec. Publ.* 5, 15–79.
- Ouwehand, P.J., 1987. Die Garschella-Formation ('Helvetischer Gault', Aptian-Cenomanian) der Churfürsten-Alvier Region (Ostschweiz) Sedimentologie, Phosphoritgenese, Stratigraphie. Ph.D. Thesis, ETH Zurich, 296 pp.
- Patterson, W.P., Walter, L.M., 1994. Depletion of $\delta^{13}\text{C}$ in seawater ΣCO_2 on modern carbonate platforms: significance for the carbon-isotopic record of carbonates. *Geology* 22, 885–888.
- Pratt, B.R., Smewing, J.D., 1993. Early Cretaceous platform margin, Oman, Eastern Arabian Peninsula. In: Simo, T., Scott, R.W., Masse, J.-P. (Eds.), *Cretaceous Carbonate Platforms*. AAPG Mem. 56, 201–212.
- Purser, B.H., 1973. Sedimentation around bathymetric highs in the southern Persian Gulf. In: *The Persian Gulf*. Springer, Berlin, pp. 335–343.
- Read, J.F., 1985. Carbonate platform facies models. *AAPG Bull.* 69, 1–21.
- Retallack, G.J., 2001. A 300-million-year record of atmospheric carbon dioxide from fossil plant cuticles. *Nature* 411, 287–290.
- Riebesell, U., Zondervan, I., Rost, B., Tortell, P.D., Zeebe, R.E., Morel, F.M., 2000. Reduced calcification of marine plankton in response to increased atmospheric pCO_2 . *Nature* 407, 364–367.
- Ruiz-Ortiz, P.A., Castro, J.M., 1998. Carbonate depositional sequences in shallow to hemipelagic platform deposits; Aptian, Prebetic of Alicante (SE Spain). *Bull. Soc. Géol. France* 169, 21–33.
- Sahagian, D., Pinous, O., Olfieriev, A., Zakharov, V., 1996. Eustatic curve for the Middle Jurassic-Cretaceous based on Russian Platform and Siberian stratigraphy: Zonal resolution. *AAPG Bull.* 80, 1433–1458.
- Schenk, K., 1992. Die Drusberg- und Schratzenkalk-Formation (Unterkreide) im Helvetikum des Berner Oberlandes. Ph.D. Thesis, University of Bern, 169 pp.
- Schlager, W., 1981. The paradox of drowned reefs and carbonate platforms. *Geol. Soc. Am. Bull.* 92, 197–211.
- Scott, R.W., 1993. Cretaceous carbonate platform, U.S. Gulf Coast. In: Simo, T., Scott, R.W., Masse, J.-P. (Eds.), *Cretaceous Carbonate Platforms*. AAPG Mem. 56, 97–109.
- Steuber, T., 2002. Plate tectonic control on the evolution of Cretaceous platform-carbonate production. *Geology* 30, 259–262.
- Tejada, M.L.G., Mahoney, J.J., Neal, C.R., Duncan, R.A., Petterson, M.G., 2002. Basement geochemistry and geochronology of Central Malaita, Solomon Islands, with implications for the origin and evolution of the Ontong Java Plateau. *J. Petrol.* 43, 449–484.
- Trabold, G.T., 1996. Development of the Urganian limestones in the Delphino Helvetic realm. *Publ. Dépt. Géol. Paléontol. Univ. Genève* 20, 187 pp.
- Vahrenkamp, V.C., 1996. Carbon isotope stratigraphy of the upper Kharaib and Shuaiba Formations; implications for the Early Cretaceous evolution of the Arabian Gulf region. *AAPG Bull.* 80, 647–662.
- Wagner, P.D., 1990. Geochemical stratigraphy and porosity controls in Cretaceous carbonates near the Oman Mountains. In: Robertson, A.H.F., Searle, M.P., Ries, A.C. (Eds.), *The Geology and Tectonics of the Oman Region*, *Geol. Soc. London Spec. Publ.* 49, 127–137.
- Ward, W.C., Brady, M.J., 1973. High-energy carbonates on the inner shelf, northeastern Yucatan Peninsula, Mexico. *Trans. Gulf Coast Assoc. Geol. Soc.* 23, 226–238.
- Weissert, H., 1989. C-isotope stratigraphy, a monitor of paleo-environmental change; a case study from the Early Cretaceous. *Surv. Geophys.* 10, 1–61.
- Weissert, H., 2000. Deciphering methane's fingerprint. *Nature* 406, 356–357.
- Weissert, H., Lini, A., Föllmi, K.B., Kuhn, O., 1998. Correlation of Early Cretaceous carbon isotope stratigraphy and platform drowning events: a possible link? *Palaeogeogr. Palaeoclimatol. Palaeoecol.* 137, 189–203.

- Wilson, J.L., Ward, W.C., 1993. Early Cretaceous carbonate platforms of Northeastern and East-Central Mexico. In: Simo, T., Scott, R.W., Masse, J.-P. (Eds.), *Cretaceous Carbonate Platforms*. AAPG Mem. 56, 35–49.
- Wissler, L., Weissert, H., Masse, J.P., Bulot, L., 2002. Chemostratigraphic correlation of Barremian and lower Aptian ammonite zones and magnetic reversals. *Int. J. Earth Sci.* 91, 272–279.
- Wortmann, U.G., Weissert, H., Funk, H., Hauck, J., 2001. Alpine plate kinematics revisited: The Adria problem. *Tectonics* 20, 134–147.
- Ziegler, M.A., 1967. A study of the Lower Cretaceous facies developments in the Helvetic Border Chain, North of the Lake of Thun (Switzerland). *Eclogae Geol. Helv.* 60, 509–527.